Received: 8 August 2016 | Revised: 7 December 2016 | Accepted: 22 February 2017

DOI: 10.1002/bio.3319

WILEY LUMINESCENCE
The Journal of Biological and Chemical Luminescence

RESEARCH ARTICLE

Luminescence, circular dichroism and *in silico* studies of binding interaction of synthesized naphthylchalcone derivatives with bovine serum albumin

Sharda Pasricha[1] | Deepti Sharma[2] | Himanshu Ojha[2] | Pragya Gahlot[1] | Mallika Pathak[3] | Mitra Basu[2] | Raman Chawla[2] | Sugandha Singhal[2] | Anju Singh[4] | Rajeev Goel[2] | Shrikant Kukreti[4] | Shefali Shukla[1]

[1] Department of Chemistry, Sri Venkateswara College, University of Delhi, Delhi, India

[2] Division of CBRN Defence, Institute of Nuclear Medicine and Allied Sciences, Delhi, India

[3] Department of Chemistry, University of Delhi, Delhi, India

[4] Nucleic Acid Research Laboratory, Department of Chemistry, University of Delhi, Delhi, India

Correspondence
Himanshu Ojha, Scientist D, Division of CBRN Defence, Institute of Nuclear Medicine and Allied Sciences, Timarpur, Delhi 110054, India.
Email: himanshu.drdo@gmail.com

Funding Information
Defence Research and Development Research

Abstract

Chalcones possess various biological properties, for example, antimicrobial, anti-inflammatory, analgesic, antimalarial, anticancer, antiprotozoal and antitubercular activity. In this study, naphthylchalcone derivatives were synthesized and characterized using ^{1}H NMR ^{13}C NMR, Fourier transform infrared and mass techniques. Yields for all derivatives were found to be >90%. Protein–drug interactions influence the absorption, distribution, metabolism and excretion (ADME) properties of a drug. Therefore, to establish whether the synthesized naphthylchalcone derivatives can be used as drugs, their binding interaction toward a serum protein (bovine serum albumin) was investigated using fluorescence, circular dichroism and molecular docking techniques under physiological conditions. Fluorescence quenching of the protein in the presence of naphthylchalcone derivatives, and other derived parameters such as association constants, number of binding sites and static quenching involving confirmed non-covalent binding interactions in the protein–ligand complex were observed. Circular dichroism clearly showed changes in the secondary structure of the protein in the presence of naphthylchalcones, indicating binding between the derivatives and the serum protein. Molecular modelling further confirmed the binding mode of naphthylchalcone derivatives in bovine serum albumin. A site-specific molecular docking study of naphthylchalcone derivatives with serum albumin showed that binding took place primarily in the aromatic low helix and then in subdomain II. The dominance of hydrophobic, hydrophilic and hydrogen bonding was clearly visible and was responsible for stabilization of the complex.

KEYWORDS

bovine serum albumin, circular dichroism, docking, luminescence, quenching

1 | INTRODUCTION

According to the World Health Organization Tuberculosis Report 2015, in 2014, there were 9.6 million cases of tuberculosis worldwide, 23% of which were in India. Currently, streptomycin, rifampicin and isoniazid are used in the treatment of tuberculosis. However, *Mycobacterium tuberculi* has developed resistance to these drugs over time; therefore, there is an urgent need to search for new potential antitubercular agents.[1]

Chalcones are well-known intermediates in the synthesis of various heterocyclic compounds. The chalcones have been reported to possess various biological properties, such as antimicrobial, anti-inflammatory, analgesic, vasorelaxant, antimalarial, anticancer, antiprotozoal, antioxidant, antihyperglycaemic, inhibition of chemical mediator release (e.g. interleukin-5, leukotriene B4, tyrosinase and aldose reductase), and antitubercular activities.[2]

Abbreviations used: ADME, Absorption, distribution, metabolism and excretion; Arg, Arginine; Asp, Aspartic acid; BSA, Bovine serum albumin; 2D, Two-dimensional; CD, Circular dichroism; Cys, Cysteine; Glu, Glutamic acid; FTIR, Fourier transform infrared; Leu, Leucine; Lys, Lysine; NMR, Nuclear magnetic resonance spectroscopy; Phe, Phenylalanine; Pro, Proline; Trp, Tryptophan; UV, Ultraviolet; Val, Valine; Vis, Visible

 Copyright © 2017 John Wiley & Sons, Ltd.

Various chalcones with naphthalene, pyrrole, piperizine, benzoazepine, morpholine and similar heterocyclic rings have been reported to have antitubercular activity. Natural-derived chalcone licochalcone 1, obtained from *Glycyrrhiza inflate*, has shown antibacterial activity against *M. tuberculosis*, *M. avium* and *M. bovis*.[3] Lipophilic chalcones and their conformationally restricted styrenylchromanones have strong antitubercular potential.[4] Some triazole methyl chalcones are known to show >80% inhibition of recombinant *M. aurum* bacteria.[5] Currently, a new series of naphthylchalcones have been reported as inhibitors of *M. tuberculosis*, targeting protein tyrosine phosphatases as more effective antitubercular agents.[6] Based on Scheme 1, some naphthylchalcones were synthesized and characterized using nuclear magnetic resonance (^{1}H NMR and ^{13}C NMR), Fourier transform infrared (FTIR) and mass techniques.

Serum albumin is the most abundant protein in the circulatory system and also the most widely studied. It has a wide range of physiological functions involving the binding, transport and deposition of many endogenous and exogenous ligands present in blood. Bovine serum albumin (BSA) has 583 amino acid residues in a single polypeptide chain cross-linked with 17 disulfide bonds. It has three homologous domains (I–III), each comprising of two subdomains (A and B).[7] The two tryptophan (Trp) residues of BSA contribute significantly to its intrinsic fluorescence; Trp134 is located in domain IB and Trp212 is buried in a hydrophobic pocket in domain IIA.[8]

It is well accepted that many drugs bind to serum albumin, and their bioavailability and efficacy depend on their binding ability.[9] Hence, the interaction between ligand and serum albumin is important in understanding drug bioavailability and efficacy. In this study, the interaction between naphthylchalcone derivatives and BSA was investigated using fluorescence spectroscopic techniques, circular dichroism (CD) and molecular docking under physiological conditions. Fluorescence quenching is often used to monitor molecular interactions and to study the mechanism of binding between drugs and plasma proteins because of its high sensitivity, reproducibility and relative ease of use.[10] The binding constants and number of binding sites were determined from the double logarithm equation. Molecular docking revealed the nature of the binding sites, as well as the prevalence of different types of interactions involved in binding. Furthermore, an absorption, distribution, metabolism and excretion (ADME) study was performed to confirm the suitability of naphthyl derivatives for use as drugs by analysing their physiochemical properties and applying Lipinski's rule of five.

This work will further help in the design and synthesis of new improved chalcone-based derivatives with better inhibitory and pharmacological actions.

2 | EXPERIMENTAL

2.1 | Materials

BSA (Fraction V, ~ 99%; protease free and essentially γ-globulin free), acetophenone (≥ 98% purity), 1-naphthaldehyde (≥ 95% purity), 2-naphthaldehyde (≥ 98% purity), methanol (≥ 99.9% purity), KOH (≥ 85% purity), ferric chloride (≥ 99.9% pure), diethyl ether (≥ 99.5% pure) and hexane (≥ 99%) were purchased from Sigma Aldrich (USA). Potassium dihydrogen phosphate (KH_2PO_4), dipotassium hydrogen phosphate (K_2HPO_4) and silica precoated alumina plates (200 μm thick) were purchased from E-Merck (Germany) and labelled actual mass fraction purities were >99%. HCl was from Thermo Fischer Scientific (India). The water used to prepare solutions was 18 MΩ MQ grade derived from a Millipore water system (model Elix 3, Millipore Corp., USA). BSA protein stock solution was prepared in 10 mM phosphate buffer (pH 7.4) and the protein solution was dialyzed overnight using dialysis cellulose membrane against the same phosphate-buffered saline at 277 K. Its concentration was determined using UV/vis absorption measurement, using the extinction coefficient of ε_{280nm} 6.60 ± 0.02. Stock solutions (1 mM) of all naphthylchalcone derivatives were prepared in methanol.

2.2 | Synthesis of naphthylchalcone derivatives

A series of four chalcones (Table 1).were synthesized by Aldol condensation between acetophenone (1.0 mM) and 1-naphthaldehyde or 2-naphthaldehyde (1.0 mM) in methanol and KOH (50% *w*/*v*) at room temperature with magnetic agitation for 24 h; the volume of KOH varied according to the reaction. On completion of the reaction, the reaction mixture was cooled on ice and then acidified with 10% HCl. The crude product was obtained by vacuum filtration and recrystallized from alcohol (Figure 1).[4] The purity of the sample was analysed using thin layer chromatography using 200-μm thick Merck silica precoated alumina plates, with solvent systems of different polarities. The desired products were obtained with an average yield of >90% after purification. Their structures were established using FTIR, NMR and mass spectrometry. ^{1}H NMR spectra showed that only E-chalcones were obtained. Other spectral data for the synthesized compounds are presented in Figures S1–S3. The general structure of naphthylchalcones is shown in Figure 2 and their substitution patterns are given in Table 1.

2.3 | Fluorescence measurements

Fluorescence steady-state measurements were performed on a spectrofluorimeter (FS920, Edinburgh Instruments, UK) with a standard 3.5 ml quartz cell. The experiment was conducted at 298 K. The excitation source was a xenon lamp (450 W) and the sample chamber was equipped with a Peltier Accessory. Scanning parameters for all measurements were optimized with a slit width of 3.0 nm for excitation and emission, a dwell time of 0.2 s and a wavelength step of 0.5 nm. The protein concentration was kept at 7.5 μM and the ligand concentrations were varied from 0 to 32.25 mM for titration. The excitation wavelength was set at 295 nm to selectively excite the Trp residues of BSA. The emission spectra were recorded over a wavelength range of 310–450 nm at a scan rate of 100 nm min^{-1} in the absence and presence of naphthylchalcone derivatives.

2.4 | CD measurements

Alterations in the secondary and tertiary structure of the protein in the presence of BSA were studied on a CD spectropolarimeter (J815, Jasco, Japan) equipped with a Peltier Accessory. The spectropolarimeter was

TABLE 1 Substitution patterns of the naphthylchalcone derivatives

Compound	IUPAC name	R^1	R^2	R^3	R^4	R^5
1a	1-(2,5-dimethoxy-phenyl)-3-naphthalen-1-yl-propenone	OCH_3	H	H	OCH_3	H
1c	1-(3-bromo-phenyl)-3-naphthalene-1-yl-propenone	H	H	H	H	Br
1d	1-(2_hydroxy-phenyl)-3-naphthalene-1-yl-propenone	OH	H	H	H	H
2a	1-(2,5-dimethoxy-phenyl)-3-naphthalene-2-yl-propenone	OCH_3	H	H	H	H

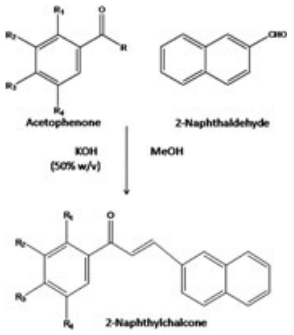

FIGURE 1 Synthesis of naphthylchalcones (Scheme 1)

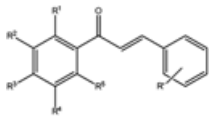

FIGURE 2 General structure of naphthylchalcone

sufficiently purged with 99.9% dry nitrogen before measurement. For CD measurements, the protein concentration and path lengths used were 1 μM and 0.1 cm, respectively. The spectra were collected at a scan rate of 50 nm min^{-1}, and a response time of 1 s. Each spectrum was baseline corrected, and the final plot was taken as an average of three accumulated plots in the range of 200–300 nm. The concentration of all naphthylchalcone derivatives was kept at 40 μM. Molar ellipticity [θ] was calculated from the observed ellipticity Θ as given in equation 1:

$$[\Theta] = 100\ x\ (\theta / c \times l) \quad (1)$$

where c is the concentration of the protein in μM and l is the path length of the cell (cm). Changes in [Θ] of each protein sample were measured at 298 K.

2.5 | Molecular docking

Molecular docking was performed by using Glide module suit Schrödinger Maestro 9.2. Glide (Grid-based ligand docking with energetic) is designed to assist in the screening of potential ligands based on binding mode and affinity for a given receptor.

The crystal structure of BSA (PDB ID: 4JK4) was obtained from the PDB database (www.rcsb.org) and the ligand structures were drawn using ChemDraw and geometry optimized using Gaussian software.

Studies were carried out at the DFT level with Gauss View 5.0 molecular visualization program and Gaussian 2009 program package. The molecular structure of naphthylchalcone derivatives in the ground state was optimized using Becke's three-parameter exchange functional (B3), which is a linear combination of Hartree Fock, local and gradient-corrected exchange terms. The B3 hybrid functional was used with the LYP correction (B3LYP), which is the correlation functional of Lee, Yang and Parr. The basis set used for calculations was the Pople's polarization 6-311G ++(d,p) basis.[11]

The protein structure was subjected to refinement using the protein preparation wizard of the Schrödinger suite in which hydrogen bonds and missing side chains in the protein structure were optimized. Co-crystallized water compounds beyond 5 Å of the active site were removed and hydrogen atoms were added to the structure by applying an all-atom force field. Protein structure was further refined using a restrained molecular mechanics calculation with the OPLS_2005 force field to remove potential steric clashes. The energy minimization of the structure was performed until the average root mean square deviation of the non-hydrogen atoms reached 0.3.

The receptor grid was generated by using a receptor grid generation program. After import of optimized structure of ligands and generation of the grid on the prepared protein, the docking calculations were performed.

Glide provides three different level of docking precision (HTVS, high-throughput virtual screening; SP, standard precision; and XP, extra precision). In this study, the XP mode of the docking program was selected for docking of different ligands with the target protein.[12,13]

2.6 | ADME screening

The QikProp program from Schrödinger Maestro 9.2[14] was used to obtain the ADME properties of the analogues. It predicts both physically significant descriptors and pharmaceutically relevant properties.

The program was processed in the normal mode, and 44 properties were predicted for the seven naphthylchalcone derivatives. These properties consisted of principal descriptors and physiochemical properties with detailed analysis of the predicted octanol/water partition coefficient (QlogPo/w), octanol/gas partition coefficient (QPlogPoct), water/gas partition coefficient (QlogPw), polarizability in cubic Å (QPolrz), % human absorption in the intestines (QP%), brain/blood partition coefficient (QPlogBB), IC_{50} value for blockage of HERG K^+ channels (logHERG), skin permeability (QPlogKp), binding to human serum albumin (QPlogKhsa), apparent Caco-2 cell permeability in mm/s (QPPCaco), and apparent MDCK cell permeability in mm/s (QPPMDCK). Caco-2 cells are a model for the gut–blood barrier, whereas MDCK cells are considered to be good mimics for the blood–brain barrier. It also evaluates the acceptability of the analogues based on Lipinski's rule of five,[15] which is essential for rational drug

design. Poor absorption or permeation is more likely when a ligand violates Lipinski's rule of five, i.e. has more than five hydrogen donors, the molecular weight is >500, logP is >5 and the sum of N and O molecules is >10.

3 | RESULTS AND DISCUSSION

3.1 | Chemistry

Purified naphthylchalcone derivatives were obtained in yields of >90%. Their structures were identified using FTIR, NMR and elementary analyses. Melting points were determined with a Microquimica MG APF-301 apparatus and are uncorrected. Infrared (IR) spectra were recorded with a FT Perkin Elmer 16 PC spectrometer on KBr disks. NMR (^{1}H and ^{13}C NMR) spectra were recorded on a Brucker Ac-200 F (200 MHz) with tetramethylsilane as an internal standard. Elementary analyses were obtained on a Perkin Elmer 2400. Percentages of C and H were in agreement with the product formula (within ±0.4% of theoretical values). The purity of the synthesized substances was analysed using thin-layer chromatography with 200-μm thick Merck silica precoated aluminium plates with several solvent systems of different polarities. Compounds were visualized with UV light (254 nm), using ferric chloride solution followed by heat as the developing agent, and purified by recrystallization from diethyl ether and hexane. ^{1}H NMR spectra revealed that all the naphthylchalcone derivatives were geometrically pure and configured E (JHa–Hb = 15–16 Hz).[16]

3.1.1 | Compound 1: (2E)-1-(2′,5′-dimethoxyphenyl)-3-(1-napthyl)-2-propen-1-one

Yellow solid, mp 89–90°C. ^{1}H NMR ($CDCl_3$, δ in ppm): 3.85 (s, 3H, OCH_3), 3.77 (s, 3H, OCH_3), 7.14 (d, 1H J = 8.2 Hz, H4′), 7.15 (dd, J = 8 Hz, 1H, H4), 7.55–7.65 (m, 5H, H3, H5, H6, H7, H8), 7.99 (d, 1H, J = 7.2 Hz, H3′), 8.01 (d, 1H, J = 16 Hz, Hα), 8.33 (s, 1H, H6′), 8.04 (d, 1H, J = 8.0 Hz, H2), 8.19 (d, 1H, J = 16.0 Hz, Hβ). IR ν_{max} cm^{-1} 1657 (C = O), 1588 (C = C), 1223, 1043 (C–O), 2947, 1493, 977, 807, 787 (KBr) .^{13}C NMR ($CDCl_3$, δ ppm): 56.12 (OCH_3), 56.72 (OCH_3), 113.60 (C3′), 114.72 (C6′), 119.71 (C4′), 123.85 (Ca), 125.40 (C1′) 125.72 (C10), 126.45 (C3), 127.06 (C9), 128.96 (C5), 129.69 (C4), 129.86 (C8), 130.72 (C6), 132.01 (C2), 132.85 (C7), 133.96 (C1), 140.20 (Cb), 152.97 (C5′), 153.90 (C2′), 192.45 (C = O). Anal. calcd for $C_{21}H_{18}O_3$ (318.36) calc. C: 79.22; H 5.69; O: 15.07; found C: 79.20; H: 6.10.

3.1.2 | Compound 2: 1-(3-bromo-phenyl)-3-napthalene-1-yl-propenone

Yellow solid, mp 89–90°C. ^{1}H NMR ($CDCl_3$, δ in ppm) 6.97 (dd, 1H, J = 7.4 Hz, H5′), 7.06 (d, 1H, J = 8.4 Hz, H3′), 7.57–7.68 (m, 4H, H3, H6, H7, H4′), 8.01 (d, 1H, J = 8.4 Hz, H3′), 7.84–7.99 (m, 4H, H6′, H4, H5, H8), 8.99 (d, 1H, J = 8.4 Hz, H2), 8.79 (d, 1H, J = 15.2 Hz, Hb), 12.88 (S, 1H, OH), ^{13}C NMR ($CDCl_3$, δ ppm): 1183.93 (C3′), 119.17 (C5′), 122.99 (Ca), 123.67 (C3), 125.59 (C8), 125.68 (C1′), 126.67 (C3), 127.41 (C6), 129.07 (C4, C5), 130.00 (C9, C6′), 131.48 (C10), 136.74 (C1, C4′), 142.66 (Cb), 163.93 (C2′), 194.12 (C = O). Anal. calcd for $C_{19}H_{14}O_2$ (274.31) calc. C: 83.19; H 5.1; O: 11.66; found C: 83.78; H: 5.17.

3.1.3 | Compound 3: 1-(2-hydroxy-phenyl)-3-napthalene-1-yl-propenone

Yellow solid, mp 106–108°C. ^{1}H NMR ($CDCl_3$, δ in ppm) 6.97 (dd, 1H, J = 7.4 Hz, H5′), 7.06 (d, 1H, J = 8.4 Hz, H3′), 7.51–7.62 (m, 4H, H3, H6, H7, H4′), 7.76 (d, 1H, J = 8.4 Hz, H3′), 7.90–7.99 (m, 4H, H6′, H4, H5, H8), 8.29 (d, 1H, J = 8.4 Hz, H2), 8.79 (d, 1H, J = 15.2 Hz, Hb), 12.88 (S, 1H, OH), IR ν_{max} cm^{-1} 1635 (C = O), 1576 (C = C), 1203, 1015 (C–O), 3047, 3451, 1351, 1435, 972, 1162, 760 (Ar) (KBr).^{13}C NMR ($CDCl_3$, δ ppm) d 1183.93 (C3′), 119.17 (C5′), 122.99 (Ca), 123.67 (C3), 125.59 (C8), 125.68 (C1′), 126.67 (C3), 127.41 (C6), 129.07 (C4, C5), 130.00 (C9, C6′), 131.48 (C10), 136.74 (C1, C4′), 142.66 (Cb), 163.93 (C2′), 194.12 (C = O). Anal. calcd for $C_{19}H_{13}OBr$ (337.21); calc. C: 67.67; H: 3.88; O: 4.74; Br: 23.73; found C: 67.58; H: 3.80.

3.1.4 | Compound 4: 2E-1-(2′,5′-dimethoxyphenyl)-3-(2-napthyl)-2-propen-1-one

Light yellow solid, mp 120–121°C. ^{1}H NMR ($CDCl_3$, δ in ppm) d 3.83 (s, 3H, OCH_3), 3.89 (s, 3H, m-OCH_3), 6.97 (d, 1H J = 8.0 Hz, H4′), 7.06 (d, J = 8.0 Hz, 1H, H3′), 7.23 (s, 1H, H6′), 7.51–7.53 (m, 2H, H6, H7), 7.53 (d, 1H, J = 16.0 Hz, Ha), 7.75 (d, 1H, J = 8.0 Hz, H3), 7.81 (d, 1H, J = 16.0 Hz, HB), 7.83–7.88 (M, 3H, H4, H5, H8), 7.99 (S, 1H, H1). IR ν_{max} cm^{-1} 1644 (C = O), 1570 (C = C), 1336, 1130 (C–O), 3012, 2946, 2837, 1508, 1227, 1005, 693(Ar) (KBr). ^{13}C NMR ($CDCl_3$, δ ppm) 55.89 (OCH_3), 56.56 (m-OCH_3), 113.42 (C3′), 109.77 (C6′), 114.40 (C4′), 123.76 (Ca), 119.17 (C1′) 132.66 (C10), 126.68 (C3), 133.36 (C9), 127.78 (C5), 130.51 (C4), 128.63 (C8), 127.07–127.23 (C6, C7), 134.27 (C2), 143.46 (Cb), 152.58–153.64 (C2′, C5′), 192.48(C = O). Anal. calcd for $C_{21}H_{18}O_3$ (318.36); calc. C: 79.22; H: 5.69; O: 15.07; found C: 79.14; H: 6.00.

3.2 | Fluorescence spectral measurements

For macromolecules, intrinsic fluorescence gives information about their structure and dynamics. Fluorescence quenching is the decrease in the fluorescence intensity of a fluorophore due to ground state complex formation, excited state reaction, energy transfer, collision quenching and molecular rearrangements.[17] Figure 3 shows the typical fluorescence band for BSA around 336 nm.[17] On subsequent addition of the naphthylchalcone derivatives, a significant decrease in the emission intensity of BSA was observed. A red shift in the wavelength maxima of 4 nm was observed for naphthylchalcone derivative **2a**, whereas in the case of naphthylchalcone derivatives **1a**, **1c** and **1d**, blue shifts in the wavelength maxima of 11, 6 and 4, respectively, were observed. The red shift suggested an increase in the polarity of the microenvironment around the Trp residues after binding of ligands with BSA. It was probably due to loss of the compact structure of hydrophobic subdomain IIA.[18–22] Therefore, it can be inferred that the binding interaction between naphthylchalcone derivative **2a** and BSA resulted in enhancement of the hydrophilicity around the Trp residues of BSA. The blue shift suggested that the Trp residue is buried in the hydrophobic environment of the BSA protein, which signifies that

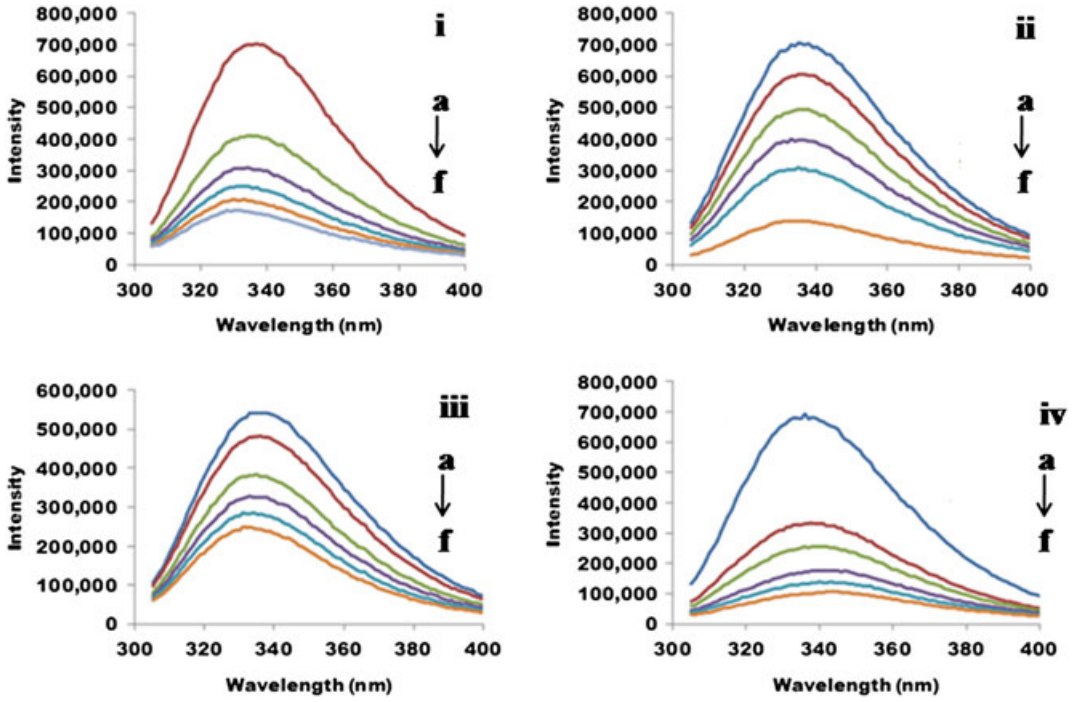

FIGURE 3 Fluorescence emission spectra of BSA [7.5 μM] in the presence of naphthylchalcone derivatives (i) 1a, (ii) 1c, (iii) 1d and (iv) 2a. The concentration of each naphthylchalcone derivatives varied from (a) 0, (b) 6.62, (c) 13.15, (d) 19.6, (e) 25.97 and (f) 32.25 μM

binding of the ligands creates a more apolar environment around the Trp residue.[23–25] Some previous studies have reported the binding of chalcones with serum proteins, but most have reported a blue shift in the wavelength maxima in the fluorescence emission spectra of the serum protein.[26,27] The shift in the wavelength maxima of BSA in the presence of naphthylchalcone derivatives suggests their binding to BSA.

Fluorescence quenching was further analysed using the Stern-Volmer equation:

$$F_0/F = 1 + K_{SV}[Q] \quad (2)$$

where, F_0 and F are the fluorescence intensities in the presence and absence of quencher, respectively, K_{SV} is the Stern-Volmer quenching constant and [Q] is the concentration of quencher.

The Stern-Volmer plots for all four derivatives are shown in Figure 4 and the obtained K_{SV} values are given in Table 2.

Molecular contact between the fluorophore and quencher is necessary in both static and dynamic quenching. In dynamic quenching, quencher must interact with the fluorophore during the excited state lifetime and no permanent change occurs during this type of quenching. But, in static quenching, a non-fluorescent complex is formed between fluorophore and a quencher on contact. [17]

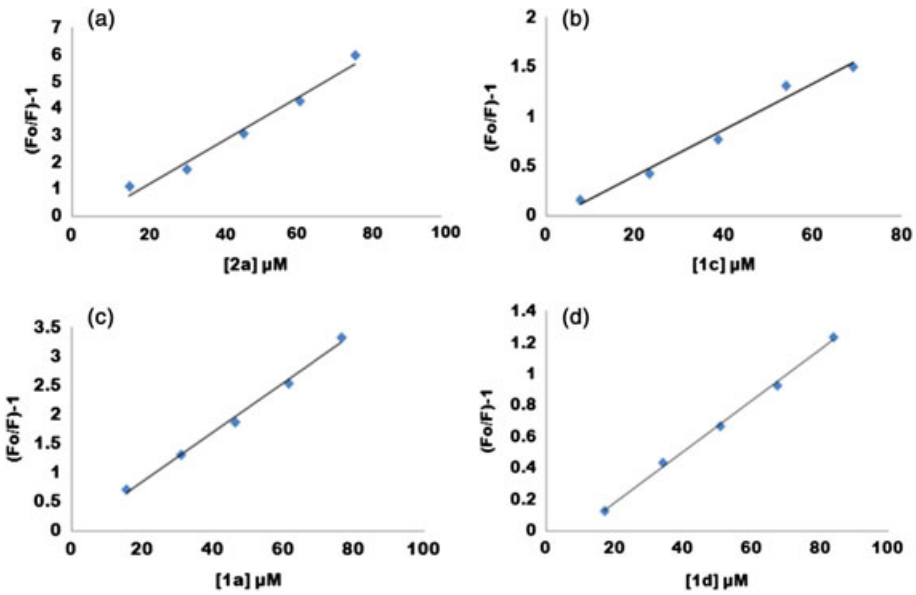

FIGURE 4 Stern–Volmer plots F_0/F versus [Q] for the binding of BSA with naphthylchalcone derivatives, (a) 2a, (b) 1c, (c) 1a and (d) 2a

TABLE 2 Association constant (*K*, *n*) and stern–Volmer quenching constant (K_{SV}) values obtained for binding of naphthylchalcone derivatives **1a**, **1b**, **1c** and **2a** for bovine serum albumin using fluorescence quenching method

Complex	K_{SV} (10^4) M^{-1}	K (10^6) M^{-1}	N
2a	8.02	1.61	1.07
1c	5.63	0.82	1.335
1a	4.23	0.26	0.952
1d	1.62	0.79	1.419

In order to establish whether the quenching mechanism is dynamic or static, the bimolecular quenching rate constant value was obtained from equation 3.

$$F_0/F = 1 + K_{SV}[Q] = 1 + k_q\tau_0[Q] \quad (3)$$

where, k_q is the second-order bimolecular quenching rate constant, τ_0 is the lifetime of excited Trp residues in BSA in the absence of quencher and K_{SV} is the Stern-Volmer constant. The τ_0 value for Trp in proteins is usually around 10^{-9} s.[17] Putting the values of K_{SV} and τ_0 for the Trp residue in equation 3, the value of k_q obtained was in order of 10^{13} M^{-1} s^{-1}. The value of k_q depends on collision between the fluorophore and quencher and its probability depends on their rate of diffusion (*D*), size and concentration. It can be shown that

$$k_q = 4\pi aDN_a \times 10^3 \quad (4)$$

where, *D* is the sum of the diffusion coefficients of quencher and fluorophore, *a* is the sum of molecular radii and N_a is the Avogadro's number. The upper limit of k_q for a diffusion-controlled process is 10^{10} M^{-1} s^{-1}.[17] In the current study, the value of k_q was 1000 to 10^{10} M^{-1} s^{-1}, hence it confirms that the quenching is essentially static in nature.[25,28]

3.3 | Analysis of binding equilibria

When small molecules bind independently to a set of equivalent sites on a macromolecule, equilibrium between the free and bound molecules is established. The association constant (*K*) and number of binding sites (*n*) for the naphthylchalcone derivative–BSA interaction were determined according to Feng *et al.*[29] using equation 5,

$$\log(F_0{-}F)/F = \log K + n\log[\mathbf{Q}] \quad (5)$$

where *K* and *n* are the association constant and the number of binding sites, respectively. A linear plot between $\log(F_0 - F)/F$ and log[complex] was observed for all four derivatives (Figure 5).

The binding parameters obtained from the plot of $\log(F_0 - F)/F_0$ against log[Q] for each of the naphthylchalcone derivatives binding with BSA are given in Table 2.

The values of *n* are ~1 for all the naphthylchalcone derivatives, which emphasizes that there is only one equivalent site in BSA for the binding of naphthylchalcone derivatives. The magnitude of the association constant, *K* (10^6) suggests a role for non-covalent binding interactions in the complexation of BSA with naphthylchalcone derivatives.[30,31] Similarly, Naik and Nandibewoor[32] reported the binding of BSA with chalcone using the fluorescence quenching method. The reported values of *n* and *K* for binding of chalcone with BSA were of the same order of magnitude as the values reported here. Therefore, thorough analysis of the fluorescence data clearly suggest the binding of naphthylchalcones with BSA.

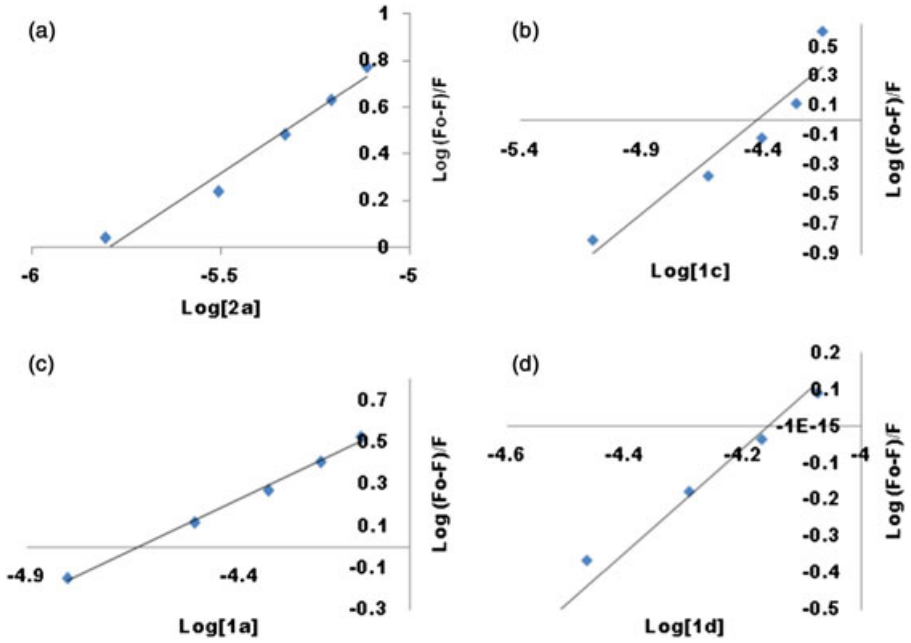

FIGURE 5 The plot of $\log(F_0{-}F)/F_0$ against log[Q] to determine the value of association constant and number of binding site of BSA with naphthylchalcone derivatives (a) 2a, (b) 1c, (c) 1a and (d) 1d respectively

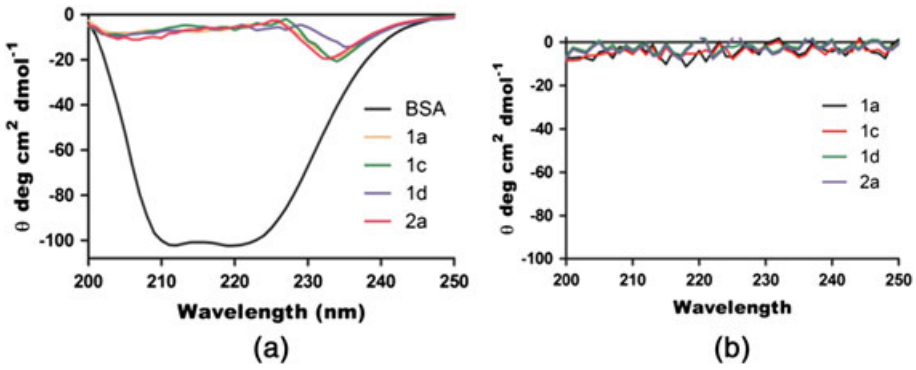

FIGURE 6 a) Circular dichroism spectra of BSA (1 μM) in the presence of 40 μM each with naphthylchalcone derivatives (1a, 1c, 1d and 2a); b) Circular dichroism spectra of 40 μM naphthylchalcone derivatives (1a, 1c, 1d and 2a)

TABLE 3 GlideScore and other detailed parameters values of the naphthylchalcone compounds (**2a**, **1a**, **1c** and **1d**) at the three different binding sites

Compound	Site	Minimization converged OPLS-2005	Docking score	Glide evdw	Glide energy	Glide einternal	Glide emodel	XP HBond
	Aromatic low helix (115–184)							
2a		0.0169	−7.3829	−1.4822	10.8891	−37.1077	−0.5361	−0.3076
1c		0.0207	−9.0279	−2.6214	9.2283	−46.3070	−0.5083	−0.3761
1a		0.0119	−8.2146	−1.5175	15.0231	−48.1499	−0.6242	−0.3422
1d		0.0003	−8.9169	0.9171	5.3734	−38.7695	−0.7	−0.4246
	Sudlow I (198–582)							
2a		0.0169	−5.1437	−0.2479	4.0687	−49.6995	0	−0.2143
1c		0.0207	−4.4882	1.7591	3.0826	−32.3191	0	−0.1870
1a		0.0119	−3.9796	1.9437	10.8729	−33.1240	−0.2770	−0.1658
1d		0.0003	−3.9071	−7.0765	1.1343	−49.3145	−0.48	−0.1860
	Sudlow II (307–582)							
2a		0.0169	−3.2807	−1.0148	0.5395	−31.8181	−0.2495	−0.1366
1c		0.0207	−3.998	−3.2669	7.0975	−43.0629	−0.5360	−0.1666
1a		0.0119	−3.6280	−3.0492	0.2172	−39.9841	−0.8813	−0.1511
1d		0.0003	−1.6744	−7.3464	3.3683	−37.0088	−1.372	−0.0797

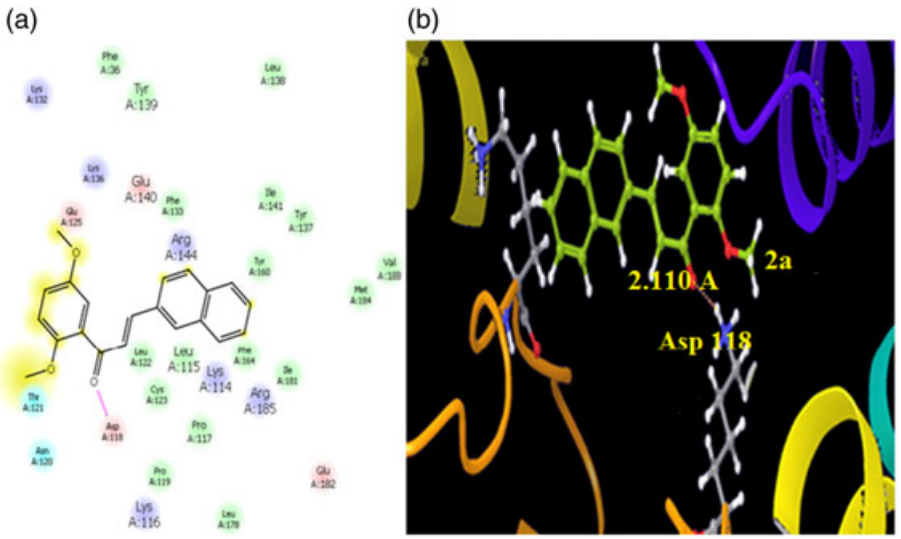

FIGURE 7 Representative 2D (a) and 3D (b) docked model of Naphthylchalcone derivative (2a) with BSA at sudlow I site

3.4 | CD studies

The CD spectra of free BSA and in the presence of 40 μM of each naphthylchalcone derivative were recorded over a wavelength range of 200–250 nm (Figure 6a). None of the synthesized derivatives show any CD signal over this wavelength range (Figure 6b). It is known that, the α helices of protein show a strong double minimum at 209 and 220 nm.[33,34] The two negative peaks at 209 and 220 nm originate in $n \rightarrow \pi^*$ transitions of the amide groups in the peptide bond and reflect the characteristic signal of the α-helical conformation of the protein.[35,36] A negative band near 222 nm is observed due to the strong hydrogen-bonding environment of the α-conformation. The intensity of this double minimum reflects the amount of helicity of BSA and indicates that BSA contains >50% helical structure. Addition of naphthylchalcone derivatives to BSA results in a decrease in the magnitude of double minimum, reflecting conformational changes leading to a decrease in α-helical content. The addition of naphthylchalcone derivatives leads to a decrease in the α-helical content of BSA from 48% to ~20%. A similar percentage decrease in the α-helical content of serum proteins in the presence of chalcones was reported by Naik and Nandibewoor[32] and He *et al.*[26] The decrease in the α-helical content of BSA clearly showed that the binding of naphthylchalcones induces changes in the secondary structure of BSA. The mechanism of α-helix unfolding may be related to gradual opening of the BSA molecule with ligands, followed by interactions between the hydrophobic sites of the protein and hydrophobic groups of ligands, resulting in subsequent changes in the protein

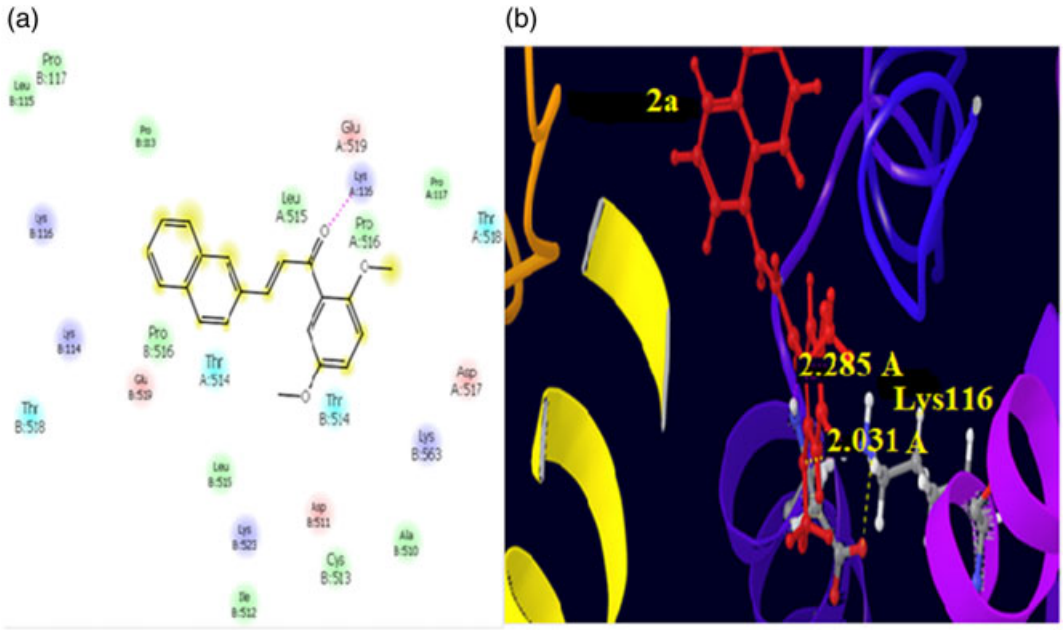

FIGURE 8 Representative 2D (a) and 3D (b) docked model of Naphthylchalcone derivative (2a) with BSA at sudlow II site

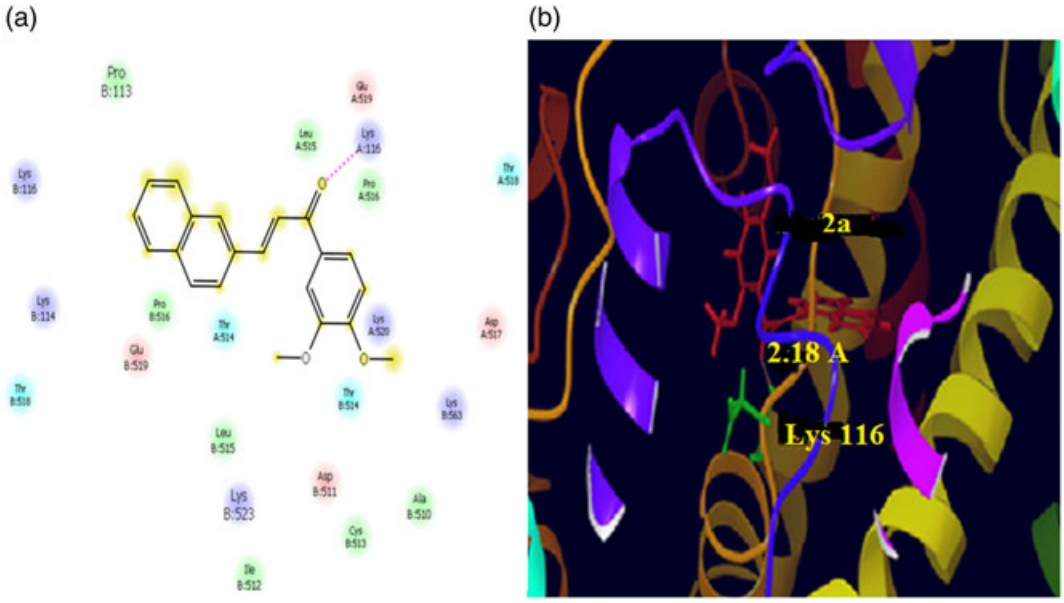

FIGURE 9 Representative 2D (a) and 3D (b) docked model of Naphthylchalcone derivative (2a) with BSA at aromatic low helix

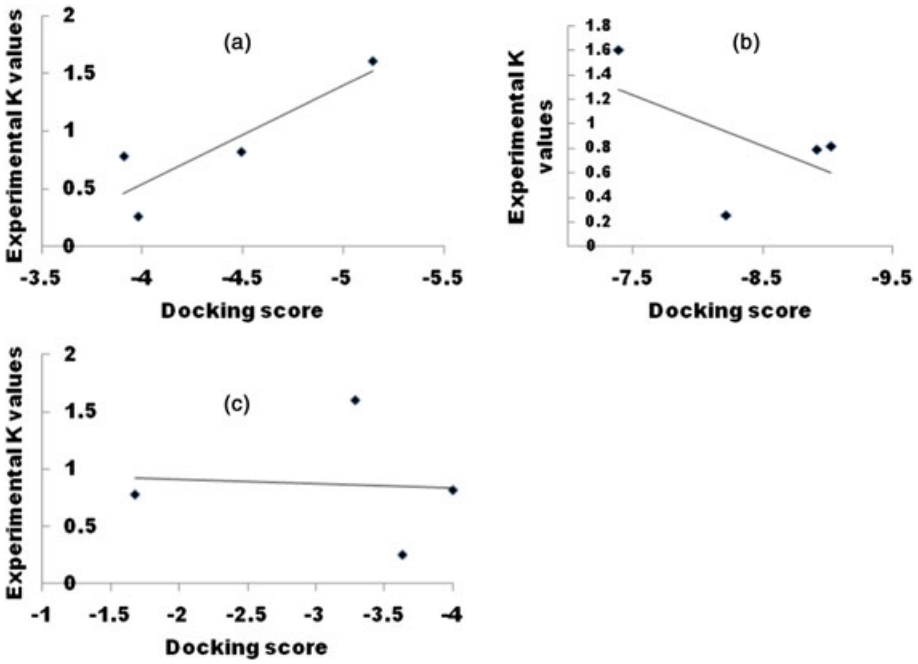

FIGURE 10 Correlation of association constant determined using fluorescence quenching study with docking score values for sites a) Sudlow I, b) Aromatic low helix and c) Sudlow I

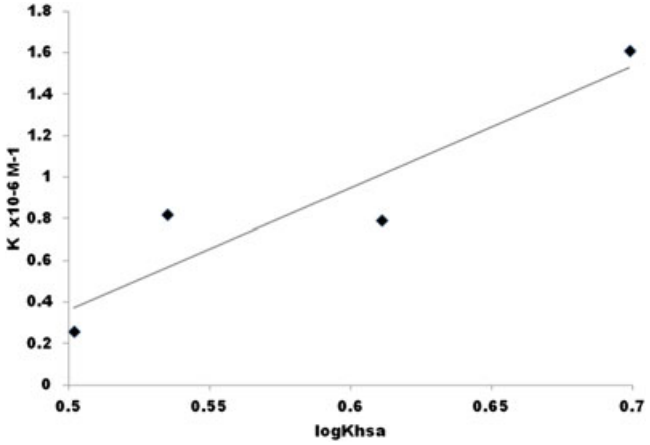

FIGURE 11 Correlation of association constant (K) versus logKhsa for compound 1a, 1c, 1d and 2a

conformation.[34] The CD studies conclude that all four synthesized naphthylchalcone derivatives bind effectively with BSA.

3.5 | Molecular docking

The binding affinity may be visualized further using a molecular docking technique. In this study, receptor PDB ID: 4J4K was docked with true structures of naphthylchalcone derivatives. The true structures of the synthesized compounds were obtained after geometry optimization based on energy minimization using Gaussian 2009 under solvent conditions. The three binding sites, aromatic low helix, Sudlow I and Sudlow II, were selected in BSA PDB based on the binding preference of the aromatic compounds in BSA.[37] The extent of binding of the ligands to the receptor protein was determined on the basis of GlideScore values.

Table 3 shows that all four ligands have diverse GlideScores ranging from −7.3829 to −9.0279 (aromatic low helix), −3.9071 to −5.1437 (Sudlow I) and −1.6744 to −3.998 (Sudlow II) in the different binding sites. Two-dimensional (2D) interaction maps suggested that in the docking site of BSA there was dominance of hydrophobic, as well as hydrogen binding, interactions. It has been reported and our previous studies indicate that both hydrophobic and hydrogen binding interactions play pivotal roles in the complexation of ligands with proteins.[24,25,28,38]

The docking scores suggested that the compounds bind to the Sudlow I site most effectively followed by Sudlow II. Compound **1c** showed the highest binding score of −9.0279 for aromatic low helix via various hydrophobic interactions with Cys513, Val554, Cys558 and Val551; ionic interactions with Asp555, Lys563, Lys556, Asp562 given in the Supporting Information.

In Sudlow I (Figure 7). Asp118 forms a hydrogen bond via a backbone with the carbonyl group of compounds. Other residues, Pro117, Leu122, Phe133 and Leu115 showed hydrophobic interactions that are common for all four ligands, whereas Glu125, Glu140, Lys116, Lys136 and Arg185 showed hydrophilic interaction with ligands. The 2D docked model of all four naphthylchalcones derivatives with BSA at Sudlow I site are given in the Supporting Information.

For Sudlow II (Figure 8). Lys116 forms hydrogen bonding via a backbone with the carbonyl group of ligand **2a**. Other residues, Pro117, Pro516 and Leu515 showed hydrophobic interactions that are common for all four ligands, whereas Gln 519 and Asp517 showed hydrophilic interaction with the ligands. The 2D docked model of all four naphthylchalcones derivatives with BSA at Sudlow II site are given in the Supporting Information.

In aromatic low helix (Figure 9). Lys116 forms a hydrogen bond via a backbone with the carbonyl group of ligand **2a**. Other residues, Cys513, Ala 560 and Ile 512 showed hydrophobic interactions that

TABLE 4 The absorption, distribution, metabolism and excretion (ADME) properties of the four naphthylchalcone derivatives

Naphthylchalcone derivative	logPo/W	logS	PCaco	logKhsa	logBB	% human oral absorption
1a	6.007	−4.85	3758.65	0.502	−0.225	91
1c	5.323	−5.52	3341.60	0.699	0.037	97
1d	5.214	−4.69	1428.75	0.611	−0.556	95
2a	6.191	−5.15	3516.28	0.535	−0.272	96

are common for all four ligands, whereas Asp517 and Lys520 show hydrophilic interaction with the ligands. The 2D docked model of all four naphthylchalcones derivatives with BSA at the aromatic low helix site are given in the Supporting Information.

Docking score values with experimentally determined association constant values using fluorescence quenching data for all the three sites are shown in Figure 10. In the case of the Sudlow I binding site, the association constant values are linearly correlated with the docking scores values. For Sudlow II, the association values are more and less linearly correlated with the docking score, except for compound **2a**. However, in the case of aromatic low helix, the experimentally determined values show poor correlation with the docking scores. Therefore, comparison of the association values with the docking score confirmed the binding of naphthylchalcone compounds in Sudlow I and II binding sites.

3.6 | *In silico* ADME prediction

To extrapolate the serum albumin ligand binding affinity, it is useful to assess the *in silico* ADME properties of the four naphthylchalcone derivatives. In ADME screening, 44 parameters are used to predict the suitability of the synthesized compounds for use as drugs. These ADME parameters include: molecular descriptors and pharmaceutically relevant properties like the partition coefficient (logPo/w) and water solubility (logS), critical for estimation of the absorption and distribution of drugs within the body; blood–brain barrier permeability (logBB), which is prerequisite for the entry of drugs into the brain; logKhsa, which predicts binding to human serum albumin, (PCaco); a model for the gut–blood barrier; the percentage of human oral absorption; and Lipinski's rule of five. These properties calculated for four compounds are given in Table 4.

None of the four derivatives violate any of Lipinski's rules, and all the derivatives have a maximum human oral absorption of >90% and allowed logKhsa values. At this point, it is also possible to compare association constant values obtained from fluorescence quenching measurements and logKhsa values obtained using *in silico* ADME prediction. A correlation coefficient value of 0.85 was obtained when logKhsa values were plotted against association constant values for the four naphthylchalcone derivatives (Figure 11).

The results suggest that good binding ability with BSA and reasonably good oral human absorption may result in better distribution and good absorption of these derivatives. The PCaco values suggest that these derivatives might have good absorption through the intestine, which is a prerequisite for better absorption of drug via the oral route. All these parameters show that these derivatives have a good potential use as drugs.

4 | CONCLUSION

The characterization of synthesized derivatives confirmed that all the naphthylchalcone derivatives obtained were E-chalcones. Fluorescence quenching of the protein in the presence of ligands was static in nature, implying the formation of a complex between naphthylchalcone derivatives and BSA. The conformational change in the BSA on binding to naphthylchalcone derivatives was confirmed by CD spectroscopy. Docking of naphthylchalcone derivatives with BSA showed strong binding at the three binding sites in the protein. The docking data showed that hydrogen bonding, hydrophobic and hydrophilic interactions are the dominant binding forces.

ACKNOWLEDGMENTS

Authors are thankful Dr A. K. Singh, Director, Institute of Nuclear Medicine & Allied Sciences, Defence Research & Development Organization for his support and thorough guidance. One of the authors Ms Deepti Sharma thanks University Grants Commission for junior research fellowship.

REFERENCES

[1] J. H. Pereira, I. B. Vasconcelos, J. S. Oliveira, R. A. Caceres, W. F. de Azevedo Jr., L. A. Basso, D. S. Santos, *Curr. Drug Targets* **2007**, *3*, 459.

[2] N. Raghav, S. Jangra, M. Singh, R. Kaur, A. Rohilla, *Int. J. Pharm. Pharm. Sci.* **2012**, *4*, 288.

[3] F. Macaev, V. Boldescu, S. Pogrebnoi, G. Duca, *Med. Chem.* **2014**, *4*, 487.

[4] I. Ahmad, J. P. Thakur, D. Chanda, D. Saikia, F. Khan, S. Dixit, A. Kumar, R. Konwar, A. S. Negi, A. Gupta, *Bioorg. Med. Chem. Lett.* **2013**, *23*, 1322.

[5] A. Ajay, V. Singh, S. Singh, S. Pandey, S. Gunjan, D. Dubey, S. K. Sinha, B. N. Singh, V. Chaturvedi, R. Tripathi, R. Ramchandran, R. P. Tripathi, *Bioorg. Med. Chem.* **2010**, *18*, 8289.

[6] A. Mascarello, M. Mori, L. D. Chiaradia-Delatorre, A. C. Orbem Menegatti, F. D. Monache, F. Ferrari, R. A. Yunes, R. J. Nunes, H. Terenzi, B. Botta, M. Botta, *PLoS One* **2013**, *8*, e77081.

[7] T. Peters, *All About Albumin: Biochemistry, Genetics, and Medical Applications*, Academic Press, San Diego **1996**.

[8] L. Trnková, I. Boušová, V. Kubíček, J. Dršata, *Nat. Sci.* **2010**, *2*, 563.

[9] M. A. Zeitlinger, H. Derendorf, J. W. Mouton, O. Cars, W. A. Craig, D. Andes, U. Theuretzbacher, *Antimicrob. Agents Ch.* **2011**, *55*, 3067.

[10] N. Wang, L. Ye, B. Q. Zhao, J. X. Yu, *Brazil J. Med. Bio. Res.* **2008**, *41*, 589.

[11] N. R. Babu, H. Saleem, S. Subashchandrabose, M. S. Padusha, S. Bharanidharan, *Spectrochim. Acta A* **2015**, *152*, 252e261.

[12] T. A. Halgren, R. B. Murphy, R. A. Friesner, H. S. Beard, L. L. Frye, W. T. Pollard, J. L. Banks, *J. Med. Chem.* **2004**, *47*, 1750.

[13] E. M. Krovat, T. Steindl, T. Langer, *Curr. Comput.-Aided Drug Des.* **2005**, *1*, 93.

[14] F. Ntie-Kang, L. L. Lifongo, J. A. Mbah, L. C. Owono, E. Megnassan, L. M. Mbaze, P. N. Judson, W. Sippl, S. M. N. Efange, *In Silico Pharmacol.* **2013**, *1*, 1.

[15] C. A. Lipinski, *J. Pharmacol. Toxicol. Methods* **2000**, *44*, 235.

[16] A. N. Choudhary, V. Juyal, *Int. J. Pharm. Pharm. Sci.* **2011**, *3*, 125.

[17] J. R. Lakowicz, *Principles of Fluorescence Spectroscopy*, Springer, New York **2004**.

[18] A. Varlan, M. Hillebrand, *Molecules* **2010**, *15*, 3905.

[19] F. L. Cui, J. Fan, J. P. Li, Z. D. Hu, *Bioorg. Med. Chem.* **2004**, *12*, 151.

[20] P. N. Naik, S. T. Nandibewoor, S. A. Chimatadar, *J. Pharm. Anal.* **2015**, *5*, 143.

[21] J. Seetharamappa, B. P. Kamat, *Chem. Pharm. Bull.* **2004**, *52*, 1053.

[22] J. Tian, J. Liu, Z. Hu, X. Chen, *Am. J. Immunol.* **2005**, *1*, 21.

[23] M. Möller, A. Denicola, *Biochem. Mol. Biol. Educ.* **2002**, *30*, 175.

[24] H. Ojha, B. M. Murari, S. Anand, M. I. Hassan, F. Ahmad, N. K. Chaudhury, *Chem. Pharm. Bull.* **2009**, *57*, 481.

[25] M. Pathak, R. Mishra, P. K. Agarwala, H. Ojha, B. Singh, A. Singh, S. Kukreti, *Thermochim. Acta* **2016**, *633*, 140.

[26] W. He, Y. Li, J. Liu, Z. Hu, X. Chen, *Biopolymers* **2005**, *79*, 48.

[27] V. Tomečková, M. Štefanišinová, B. Veliká, K. Fodor, P. Perjési, M. Stupák, J. Guzy, Š. Tóth Jr., T. Pekárová, *Spectr. Anal. Rev.* **2013**, *1*, 1.

[28] D. Sharma, H. Ojha, M. Pathak, B. Singh, N. Sharma, A. Singh, R. Kakkar, R. K. Sharma, *J. Mol. Struct.* **2016**, *1118*, 267.

[29] X. Z. Feng, Z. Lin, L. J. Yang, C. Wang, C. L. Bai, *Talanta* **1998**, *47*, 1223.

[30] H. Ojha, K. Mishra, M. I. Hassan, N. K. Chaudhury, *Thermochim. Acta* **2012**, *548*, 56.

[31] H. Aki, M. Yamamoto, *J. Pharm. Pharmacol.* **1989**, *41*, 674.

[32] K. M. Naik, S. T. Nandibewoor, *J. Lumin.* **2013**, *143*, 484.

[33] B. P. Kamat, J. Seetharamappa, *J. Photosci.* **2004**, *11*, *29*.

[34] B. P. Kamat, J. Seetharamappa, M. B. Melwanki, *Int. J. Biochem. Biophys.* **2004**, *41*, 173.

[35] H. Xu, N. Yao, H. Xu, T. Wang, G. Li, Z. Li, *Int. J. Mol. Sci.* **2013**, *14*, 14185.

[36] B. M. Bulheller, A. Rodger, J. D. Hirst, *Phys. Chem. Chem. Phys.* **2007**, *9*, 2020.

[37] T. Peters, *Adv. Protein Chem.* **1986**, *37*, 161.

[38] P. D. Ross, S. Subramanian, *Biochemistry* **1981**, *20*, 3096.

SUPPORTING INFORMATION

Additional Supporting Information may be found online in the supporting information tab for this article.

How to cite this article: Pasricha S, Sharma D, Ojha H, et al. Luminescence, circular dichroism and *in silico* studies of binding interaction of synthesized naphthylchalcone derivatives with bovine serum albumin. *Luminescence*. 2017. https://doi.org/10.1002/bio.3319